COMPARISON OF PHOTODYNAMIC THERAPY PROTOCOLS ON *IN VITRO* PERI-IMPLANTITIS MODELS

by

Ebru Saraç

BS., Biomedical Engineering, Yeditepe University, 2021

Submitted to the Institute of Biomedical Engineering
in partial fulfillment of the requirements
for the degree of
Master of Science
in
Biomedical Engineering

Boğaziçi University
2024

COMPARISON OF PHOTODYNAMIC THERAPY PROTOCOLS ON *IN VITRO* PERI-IMPLANTITIS MODELS

APPROVED BY:

Assist. Prof. Dr. Mustafa Kemal Ruhi (Thesis Advisor)	.....
Prof. Dr. Bora Garipcan	.....
Assoc. Prof. Dr. Nermin Topaloğlu Avşar	.....

DATE OF APPROVAL: 04 june 2024

ACKNOWLEDGMENTS

Firstly, I want to thank my advisor, Assist. Prof. Dr. Mustafa Kemal Ruhi. From the first minute to last, I felt very grateful for the support and guidance he gave me. I appreciate his patience and efforts to keep me motivated throughout this journey of mine.

I want to thank Prof. Dr. Bora Garipcan and the members of Biomimetic and Bioinspired Biomaterials LaBORAtory for providing me with opportunities and ideas to do my experiments.

I will indefinitely be thankful to my family for their never ending prayers, love, patience, and encouragement. Especially, I want to thank my siblings Elif and Mehmet for always being there, you are my biggest happiness in this life. Finally, I want to thank my dearest Şeyma for her solid friendship which I learned from her and feel so lucky to have.

Boğaziçi University Scientific Research Projects, No:19541, has funded this study.

ACADEMIC ETHICS AND INTEGRITY STATEMENT

I, Ebru Saraç, hereby certify that I am aware of the Academic Ethics and Integrity Policy issued by the Council of Higher Education (YÖK) and I fully acknowledge all the consequences due to its violation by plagiarism or any other way.

Name :

Signature:

Date:

ABSTRACT

COMPARISON OF PHOTODYNAMIC THERAPY PROTOCOLS ON *IN VITRO* PERI-IMPLANTITIS MODELS

Peri-implantitis is a periodontal disease characterized by soft tissue inflammation and bone tissue resorption. Increasing antibiotic resistance hinders the cure of peri-implantitis with antibiotics. In addition, mechanical and chemical interventions may disrupt the osseointegration of the implant because they can cause alterations in the surface roughness. Antibacterial photodynamic therapy is a non-invasive light-based treatment that utilizes photosensitive molecules and it is considered to be a strong alternative to cure bacterial infections. Chlorin e6 is an anionic second-generation photosensitizer. It has low cytotoxicity and high photodynamic properties however there is no study showing the antibacterial efficacy of chlorin e6 for peri-implantitis, to the author's knowledge. In this thesis, we aimed to demonstrate the antibacterial effect of chlorin e6 on both planktonic bacteria and a realistic *in vitro* peri-implantitis model. We compared the results with methylene blue as it is widely studied for peri-implantitis. Further, we utilized potassium chloride, an inorganic salt, to enhance the effect of photodynamic therapy. The results showed that methylene blue-mediated photodynamic therapy outperformed chlorin e6 on planktonic bacteria and caused almost a 6-log reduction in bacterial load. However, in the *in vitro* PI model there were no statistically significant differences between chlorin e6 and methylene blue. The highest antibacterial effect was achieved with the chlorin e6-mediated photodynamic therapy with the addition of potassium chloride. This thesis showed that chlorin e6-mediated photodynamic therapy potentiated with potassium chloride can be an alternative to methylene blue to cure peri-implantitis.

Keywords: Photodynamic Therapy, Peri-implantitis, Chlorin e6, Methylene blue, *Staphylococcus aureus*, potassium chloride.

ÖZET

İN-VİTRO PERİ-İMPLANTİTİS MODELLERİNDE FOTODİNAMİK TERAPİ PRTOKOLLERİNİN KARŞILAŞTIRILMASI

Peri-implantitis, yumuşak doku iltihabı ve kemik dokusu erimesi ile karakterize edilen periodontal bir hastalıktır. Artan antibiyotik direnci peri-implantitisin antibiyotikle tedavisini zorlaştırmaktadır. Ayrıca mekanik ve kimyasal yöntemler yüzey pürüzlülüğünde değişikliklere neden olabileceği için implantın osseointegrasyonunu bozabilmektedir. Antibakteriyel fotodinamik terapi, fotosensitizer moleküller kullanan ve bakteriyel enfeksiyonları tedavi etmek için güçlü bir alternatif olarak kabul edilen, invazif olmayan, ışık bazlı bir tedavidir. Klorin e6, anyonik, ikinci nesil bir fotosensitizerdir. Düşük sitotoksisiteye ve yüksek fotodinamik özelliklere sahiptir ancak, yazarın bilgisi dahilinde, bildirilen çalışmalar peri-implantitis tedavisinde klorin e6'nın antibakteriyel etkinliğini göstermek için yetersiz kalmaktadır. Bu tezde klorin e6'nın, hem planktonik bakteriler üzerinde hem de gerçekçi *in vitro* peri-implantitis modelinde antibakteriyel etkisini göstermeyi amaçladık. Peri-implantitis tedavisinde yaygın olarak çalışılan bir fotosensitizan olduğundan sonuçları metilen mavisi ile karşılaştırdık. Ayrıca tedavi sonuçlarını iyileştirmek için inorganik bir tuz olan potasyum klorürden faydalandık. Sonuçlar metilen mavisi aracılı fotodinamik tedavinin planktonik bakteriler özerinde klorin e6'dan daha iyi performans gösterdiğini ve bakteri yükünde 6-log azalmaya neden olduğunu gösterdi. Ancak gerçekçi *in vitro* modelde klorin e6 ile metilen mavisi arasında istatistiksel olarak anlamlı bir fark görülmedi. En yüksek antibakteriyel etki, klorin e6 aracılı fotodinamik terapi ve potasyum klorür ilavesiyle elde edildi. Bu tez, potasyum klorürle güçlendirilen klorin e6 aracılı fotodinamik tedavinin peri-implantitis tedavisinde metilen mavisine alternatif olabileceğini gösterdi.

Anahtar Sözcükler: Fotodinamik terapi, Peri-implantitis, Klorin e6, Metilen mavisi, *Stafilakok aureus*, potasyum klorür

TABLE OF CONTENTS

ACKNOWLEDGMENTS iii
ACADEMIC ETHICS AND INTEGRITY STATEMENT iv
ABSTRACT v
ÖZET vi
LIST OF FIGURES ix
LIST OF TABLES xii
LIST OF SYMBOLS xiii
LIST OF ABBREVIATIONS xiv
1. INTRODUCTION 1
1.1 Motivation 1
1.2 Aim of the Thesis 3
2. BACKGROUND 4
2.1 Peri-Implantitis and The Microbial Environment Of Peri-Implantitis . . 4
2.2 Conventional Treatment Models of Peri-implantitis 4
2.3 Antibacterial Photodynamic Therapy and the Mechanism of Action . . 6
2.4 Photosensitizers: Chlorin e6 8
2.5 Light Sources 9
2.6 Biochemical Inactivation Mechanism of aPDT 10
3. MATERIAL AND METHOD 12
3.1 Bacterial strain 12
3.2 Preparation of photosensitizer solutions 12
3.3 Preparation of potassium chloride solution 12
3.4 Assessment of bacterial viability; Colony forming unit method 13
3.5 Preparation of rough titanium discs 13
3.6 Roughness measurement of titanium discs 14
3.7 *In vitro* peri-implantitis model: Bacteria adhered on rough titanium disc. 14
3.8 Optical setup 15
3.9 Photodynamic therapy 15
3.10 SEM analysis 18

3.11 Statistical analysis 18
4. RESULTS 19
4.1 Antibacterial effect of dark toxicity of Ce6 and MB on *S. aureus* 19
4.2 Absorption spectra of Ce6 and MB 20
4.3 Antibacterial effect of 660 nm of light 21
4.4 Antibacterial effect of Ce6 and MB-mediated PDT on planktonic bacteria 22
4.5 Antibacterial effect Ce6 and MB-mediated PDT on *in vitro* PI model . 24
4.6 Antibacterial effect of the KCl addition to Ce6 and MB mediated PDT on *in vitro* PI model 25
4.7 Roughness measurements 26
4.8 SEM analysis 28
5. DISCUSSION 30
6. CONCLUSION 35
REFERENCES 36

LIST OF FIGURES

Figure 2.1	Schematic illustration of a photodynamic therapy application in clinic.	6
Figure 2.2	Schematic representation of a Jablonski diagram showing the Type 1 and Type 2 reactions of the PDT mechanism.	7
Figure 2.3	Chemical structure of Ce6.	8
Figure 2.4	Visible spectrum region of the electromagnetic spectrum.	9
Figure 3.1	Images of colony forming units on TSA plates after a PDT application.	13
Figure 3.2	Images of a) polished and b) sandblasted titanium discs.	14
Figure 3.3	Image of titanium discs placed on fresh bacterial broth solution before incubation for 48 hours.	15
Figure 3.4	Image of a 660 nm collimated LED illuminating the 12 well-plate for the PDT application.	16
Figure 4.1	Antibacterial effect of dark toxicity of 0 μM, 5 μM,10 μM, 25 μM, and 50 μM Ce6 on *S. aureus*. The number of CFUs in each group was normalized with the no treatment (0 μM) group. (*: $p<0.05$, ns: not significant).	19
Figure 4.2	Antibacterial effect of dark toxicity of 0 μM, 5 μM,10 μM, 25 μM, and 50 μM MB on *S. aureus*. The number of CFUs in each group was normalized with the no treatment (0 μM) group. (*: $p<0.05$, ns: not significant).	20
Figure 4.3	Absorption spectra of a) 25 μM Ce6 and b)5 μM MB before and after irradiation with 660 nm LED at 60 J/cm^2 and 30 J/cm^2 energy densities, respectively.	21
Figure 4.4	Effect of 660nm light irradiation on *S. aureus* suspensions at 100 mW/cm^2 power density. $0J/cm^2$, 30 J/cm^2 and 60 J/cm^2 energy densities were applied for 0, 5, and 10 minutes, respectively. The number of CFUs in each group was normalized with the no treatment group. (*: $p<0.05$, ns: not significant)	22

Figure 4.5 Antibacterial effect of 30 J/cm^2 and 60 J/cm^2 Ce6-mediated PDT on *S. aureus* suspensions. The number of CFUs in each group was normalized with the no treatment group. (*: $p<0.05$, ns: not significant) 23

Figure 4.6 Antibacterial effect of 30 J/cm^2 MB-mediated PDT on *S. aureus* suspensions. The number of CFUs in each group was normalized with the no treatment group. (*: $p<0.05$, ns: not significant) 23

Figure 4.7 Antibacterial effect of 60 J/cm^2 Ce6-medieated PDT and 30 J/cm^2 MB-medieated PDT on *S. aureus* suspensions shown on the left. The antibacterial effect of 60 J/cm^2 Ce6-mediated PDT and 30 J/cm^2 MB-mediated PDT on *in vitro* PI model is shown on the right. The number of CFUs in each group was normalized with the no treatment group. (*: $p<0.05$, ns: not significant) 24

Figure 4.8 Antibacterial effect of 60 J/cm^2 Ce6-mediated PDT with and without 400 mM KCl on *in vitro* PI model. The number of CFUs in each group was normalized with the no treatment group. (*: $p<0.05$, ns: not significant) 25

Figure 4.9 Antibacterial effect of 60 J/cm^2 MB-mediated PDT with and without 400 mM KCl on *in vitro* PI model. The number of CFUs in each group was normalized with the no treatment group. (*: $p<0.05$, ns: not significant) 26

Figure 4.10 3D digital microscope images of random a) polished, and b) sandblasted titanium disc 1 and c) sandblasted titanium disc 2 and d) sandblasted titanium disc 3. 27

Figure 4.11 SEM images of bacteria forming clusters on a) sandblasted titanium disc and b) polished titanium disc. 28

Figure 4.12 SEM images of bacteria on sandblasted titanium discs after no treatment at a1) 5000x magnification, a2) 10000x magnification; 25 μM Ce6 mediated PDT at b1) 5000x magnification, b2) 10000x magnification; 5 μM MB-mediated PDT at c1) 5000x magnification, c2) 10000x magnification at energy densities 0 J/cm^2, 30 J/cm^2 and 60 J/cm^2, respectively. 29

Figure 4.13 SEM images of bacteria on sandblasted titanium discs after a) no treatment, b) 25 μM Ce6 mediated PDT with the addition of KCl, c) 5 μM MB-mediated PDT with the addition of 400 mM KCl at energy densities 0 J/cm^2, 30 J/cm^2 and 60 J/cm^2, respectively. 29

LIST OF TABLES

Table 3.1	Parameters that will be applied on planktonic bacteria for the treatment groups of dark toxicity, light toxicity, and PDT	17
Table 3.2	Parameters that will be applied on the *in vitro* PI model for the treatment groups of PDT.	17
Table 4.1	Roughness values of the polished and sandblasted discs measured with a 3D microscope.	27

LIST OF SYMBOLS

°C	Degrees Celcius

LIST OF ABBREVIATIONS

PI	Peri-implantitis
PDT	Photodynamic therapy
aPDT	Antibacterial Photodynamic therapy
PS	Photosensitizer
MB	Methylene blue
TBO	Toluidine blue
Ce6	Chlorin e6
RB	Rose bengal
KCl	Potassium chloride
ROS	Reactive oxygen species
TSA	Tryptic soy agar
TSB	Tryptic soy broth
PBS	Phosphate buffered saline
CFU	Colony forming unit
min	minute
mL	mililiter
μL	mikroliter
mM	milimolar
μM	mikromolar
μm	mikrometer
mm	milimeter
cm	centimeter
rpm	Revolutions per minute
J	Joule
W	Watt
mW	miliwatt

1. INTRODUCTION

1.1 Motivation

Oral infections are one of the most prevalent diseases all around the world [1]. Increasing rates of infectious diseases seriously affect the economy and the health industries of underdeveloped countries [2]. Peri-implantitis (PI) is an oral infection of the soft tissue around a dental implant. It is characterized by bone resorption and reduced osseointegration of the implant [3]. The main reason for PI is that oral bacteria form a structure on dental implants made from polysaccharides called biofilm. Biofilms act as a sack for bacteria and quickly adapt resistance mechanisms to protect bacteria from external conditions [4].

Traditional treatments of PI include mechanical chemical and surgical interventions. In general, conventional treatments are used together to enhance the treatment outcomes [3, 5]. Besides conventional modalities, there are novel light-based treatments that utilize light. Photodynamic therapy (PDT) is a treatment modality that is utilized to treat cancer and bacterial infections. The PDT mechanism involves exciting a photosensitizer (PS) molecule with a specific wavelength of light. The photochemical reactions between PS and the oxygen in the environment produce reactive molecular species which destroy cells [6, 7]. Even though antibacterial PDT (aPDT) has been developed enormously in recent years, parameters such as light dose, irradiation time, PS type, and PS dosage are still being investigated to acquire reproducible PDT protocols for PI [8]. Also understanding the interaction of those parameters with laser and dental implants hardens the success of *in vivo* studies or even further the clinical applications [9]. While numerous effective studies have been conducted, the precise determination of the optimal concentration of a PS that can effectively eliminate bacteria without causing harm to human cells remains open to investigation [10]. For example, according to Jiashing *et al.*, the dark cytotoxicity of methylene blue (MB) on HeLa cells starts to increase after a concentration of 20 μM, and the effective MB dose for the

photodynamic inactivation varies from cell to cell [11, 12]. Huang *et al.* reported that the effective dose of MB is accepted to be 1 μM for *Pseudomonas aeruginosa* while for *Staphylococcus aureus* it increases up to 10 μM [12].

According to a literature search, methylene blue (MB) and toluidine blue (TBO) are commonly used PSs in antibacterial PDT (aPDT) to treat PI [13]. For example, in an *in vivo* study, Almeida *et al.* investigated the MB-mediated PDT on experimental periodontal disease which they modeled on rat mandibular teeth. Five and fifteen days after the therapy, the radiological results showed that the PDT group had fewer bone tissue loss than the controls. However, after thirty days, there were no significant differences between the groups [14]. Besides MB and TBO, another studied PS for aPDT is Chlorin e6 (Ce6). Ce6 is a second-generation PS that has been extensively studied in cancer studies and is notable for its beneficial characteristics, which include substantial absorption in the near-infrared range of the electromagnetic spectrum, high quantum yield, and low dark toxicity [15, 16]. However, studies evaluating the antibacterial potential of Ce6 for PI are few therefore need for further investigation. In a comparative investigation of the efficacy of MB and Ce6 on Streptococcus mutans biofilms, Nie *et al.* found that both compounds were effective in biofilm removal. Notably, Ce6-based PDT outperformed MB at higher concentrations. The antibacterial effect of Ce6-mediated PDT increased with increasing concentration and reduced the bacterial count by 5-log at high concentration. At lower concentrations MB-mediated PDT was more effective in killing however viability increased with increasing concentration [17]. In another study, Nie *et al.* investigated the effect of combined Ce6-mediated PDT with hydrogen peroxide, on multi-species biofilm. Their results showed that 50μM Ce6 and hydrogen peroxide synergistically decreased the bacterial load by 6.6 log [18]. Avşar *et al.* investigated the antibacterial PDT efficacy of Ce6 at lower energy density and concentration with the addition of 20% ethanol on methicillin-resistant *staphylococcus aureus* (MRSA) strain. All the PDT groups achieved a high antibacterial effect. However, addition of ethanol showed better outcomes at both lower concentration and energy density which is desirable to reduce the PS and light toxicity [19]. Besides adjunctive antibacterial agents such as ethanol and hydrogen peroxide, other strategies have been investigated to potentiate the efficacy of PDT. Utilizing non-toxic inorganic salts is

one of the investigated strategies. For example, Rose bengal (RB) is a PS that has additional dark antibacterial potential [20]. While RB-mediated PDT is effective on gram-positive bacteria, it remains less active on gram-negative strains. To increase the antibacterial effect of RB-mediated PDT on gram-negative bacteria Wen *et al.* utilized potassium iodide. Iodide groups caused chemical reactions which led to the creation of other toxic compounds such as hydrogen peroxide and molecular iodine [21]. In addition to that, our research group recently published a conference proceeding and showed that potassium chloride (KCl) addition to Ce6-mediated PDT has increased the antibacterial effect on *S.aureus* [22].

In vitro aPDT studies generally utilize glassware or well plates to examine photodynamic efficacy although the implants are generally made from titanium [23, 24]. However, more realistic *in vitro* models are necessary to mimic the physical and mechanical environment of the disease that may affect the behavior and treatment response of bacteria [25]. So far no study shows the antibacterial efficacy of Ce6-mediated PDT on a titanium surface to treat PI.

Based on this literature review, we hypothesize that Ce6-mediated PDT is an effective protocol to treat PI. In addition, we anticipate that the addition of KCl as a non-toxic inorganic salt will increase the phototoxicity created by Ce6-mediated PDT.

1.2 Aim of the Thesis

The main goal of this thesis is to demonstrate the antibacterial potential of Ce6-mediated PDT by comparing it with a more studied and reliable protocol which is MB-mediated PDT, performed on bacterial suspension and bacteria-adhered titanium discs as *in vitro* PI model under 660 nm light (Both Ce6 and MB has a peek absorbance at 660 nm). Hence the result of this study will provide valuable information to the literature about the interaction between light and bacteria on rough titanium surfaces for the future clinical application of Ce6-mediated PDT to cure PI.

2. BACKGROUND

2.1 Peri-Implantitis and The Microbial Environment Of Peri-Implantitis

Peri-implant diseases are inflammatory conditions that occur when bacteria infiltrate the tissue around dental implants. It can manifest in two different forms which are peri-implant mucositis and PI. Peri-mucositis is the infection of the soft tissue around the implant. However, in PI progressive bone tissue loss accompanies the soft tissue inflammation [3]. Diaz *et al.* reported the overall prevalence of PI. At patient level, the mean prevalence was measured as 11.96%, and at implant level, it was 12.39% [26]. At the patient level, patients with a history of Periodontitis which is gum inflammation, smoking, and poor dental hygiene contribute to the development of the disease. However, the major pathological reason for PI is the formation of the biofilm by the oral microorganisms around the implant surface and consequently the infection causes an increase in osteoclast activity [27]. The most commonly associated bacteria with PI are *Actinobacillus actinomycetemcomitan, Tannerella forsythia, Porphyromonas gingivalis*, and *Prevotella intermedia. S. aureus* is another bacteria that is gram-positive and anaerobic that is involved in the first colonizing stages of PI, and known to have a high affinity to titanium surfaces [28].

2.2 Conventional Treatment Models of Peri-implantitis

The care of the PI is more complicated when compared to other peri-implant disorders due to the complex structure of the dental implant. [29]. Even though the same treatment models are generally employed for peri-implant disorders, supportive therapies are required for PI [3]. Treatment strategies are aimed at preventing implant failure and managing infection to halt the course of the disease and ultimately restore the bone tissue [30]. Conventionally PI is treated with surgical, non-surgical, or surface

decontamination methods. The surgical methods involve resective and regenerative surgeries [3].

Non-surgical methods involve mechanical interventions, antibiotics and antiseptics. Mechanical tools such as curettes, air-abrasive tools, and ultrasonic scalers are useful to reduce inflammation by scraping the microbial plaque over the surface. Since it is hard to reach the treads of the implant by using mechanical tools, they are generally supported with systemic antibiotics or surgery [3]. Although surgery is the most powerful treatment of PI, it is a disturbing procedure that reduces patient comfort. Similarly, antibiotics have drawbacks such as systemic side effects and increasing antibiotic resistivity of the pathogens due to the overprescription and misuse [31].

Surface decontamination involves the use of antimicrobial agents topically. Chemicals such as citric acid, hydrogen peroxide, and other antimicrobial agents are applied topically to control the infection and prevent the recurrence of the disease [32]. Unlike antibiotics, they do not have any resistance to pathogens however they have their own limitations. They are highly toxic chemicals and therefore have to be used with caution to prevent any skin irritation when used topically. Also, they affect bodily cells together with bacterial cells. For instance, Liu *et al.* have shown that a clinical dose of 2% chlorhexidine dramatically lowers fibroblast, myoblast, and osteoblast survival as well as stops the cell migration permanently [33]. Antimicrobial agents can also be administered to the blood circulation. However, sustaining the therapeutic amount of drug inside the bloodstream which must reach the periodontal pocket is challenging [34]. Because of these methods cannot eradicate the entire biofilm, the remaining bacteria lead to the recurrence of the disease. Therefore, there is need for a strong alternative to those antibacterial therapies which can halt the complex microbial environment of the PI.

Besides the aforementioned modalities, light-based novel treatments such as low-high energy lasers are being investigated to treat periodontal diseases [35]. PDT is a non-invasive treatment that employs low-level lasers to kill bacteria. Unlike high-level lasers, PDT does not cause harm to the host tissue thanks to its high selectivity in

targeting bacteria and low energy dosage [34].

2.3 Antibacterial Photodynamic Therapy and the Mechanism of Action

aPDT is a treatment approach to cure antibiotic-resistant bacterial infections that utilizes PS molecules to destroy bacteria when irradiated with a specific wavelength of light. In aPDT, PS molecules are taken up by bacteria and then excited by visible light that comes from a laser source (Figure 2.1). Then PS molecules transfer their energy to molecular oxygen or other biomolecules in the environment to create free radicals and reactive oxygen species (ROS) which are toxic to bacteria [6]. Therefore, a successful PDT application requires PS, light, and oxygen in the presence.



Figure 2.1 Schematic illustration of a photodynamic therapy application in clinic [7].

Two recognized mechanisms of the photodynamic reaction is Type 1 and Type 2 reactions. Both of the reactions start with the excitation of the singlet ground state PS to the singlet excited state due to photon absorption. Then singlet excited state PS goes to triplet excited state by intersystem crossing (Figure 2.2). Triplet excited state PS has a longer lifetime compared to singlet state which has enough time to transfer its energy [36].

In the Type 1 mechanism, free radicals are produced by the electron donation between a substrate (a biomolecule in the environment) and excited triplet state PS. Then these radicals start a reaction with molecular oxygen to produce reactive oxygen molecules (ROS) such as hydroxyl radicals. As a result of these reactions oxidative stress reaches to high levels that cells can not survive. In the Type 2 reaction, excited triplet state PS directly transfers its energy to the ground triplet state molecular oxygen to produce excited singlet state oxygen which is a strong oxidizer. It is assumed that the pioneer cytotoxic effect is achieved by the Type 2 reactions and specifically by the singlet oxygen [37].

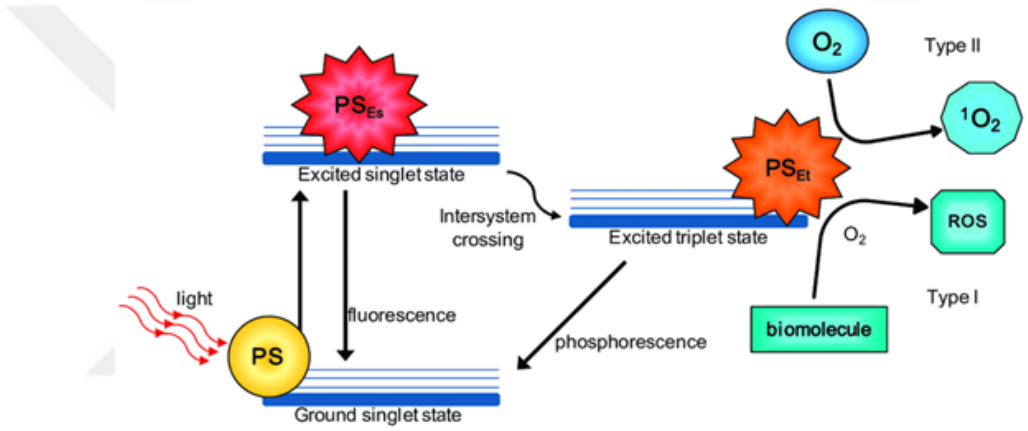

Figure 2.2 Schmetic Jablonski diagram showing the Type 1 and Type 2 reactions of the PDT mechanism [38].

This photo-activated disinfection has several advantages over conventional treatments of PI. The main advantage of PDT is the reduced systemic side effects thanks to local delivery of the PSs and light especially for superficial and localized infections [34]. Even though PDT can be applied to a specific area, there is still a small risk of killing the beneficial oral bacteria or eukaryotic cells. Many studies have developed active targeting nanocarriers to target specific organisms with high sensitivity to overcome this drawback [39]. Another important advantage of PDT is that no microorganism that has been studied has yet been able to have resistance to the unique killing mechanism of PDT [39]. In addition to that, the majority of the light sources and PSs are commercially available and can be used repeatedly which makes PDT a promising alternative [34].

2.4 Photosensitizers: Chlorin e6

A PS is a chemical compound that can absorb and transfer photon energy to increase the light sensitivity of the surroundings [40]. PS is one of the three main components for successful photodynamic activation and directly affects the treatment outcomes. Therefore they should have certain properties. Some can be listed as follows; high cellular affinity, rapid clearance from healthy cells, high singlet oxygen quantum yield, and low cytotoxicity [41]. There are several types of PSs categorized by their chemical structure and generation [42].

First-generation PSs are photofrin and hematoporphyrin derivatives. They have poor selectivity of the target tissue and a low extinction coefficient. Therefore high concentrations are being administered to achieve a therapeutic level. Over the years scientists developed second-generation PSs such as chlorins, bacteriochlorins, and phthalocyanines. In general, they are stronger in terms of targeting selectivity, ROS production, longer absorption range, better tissue penetration, and low systemic side effects [42].

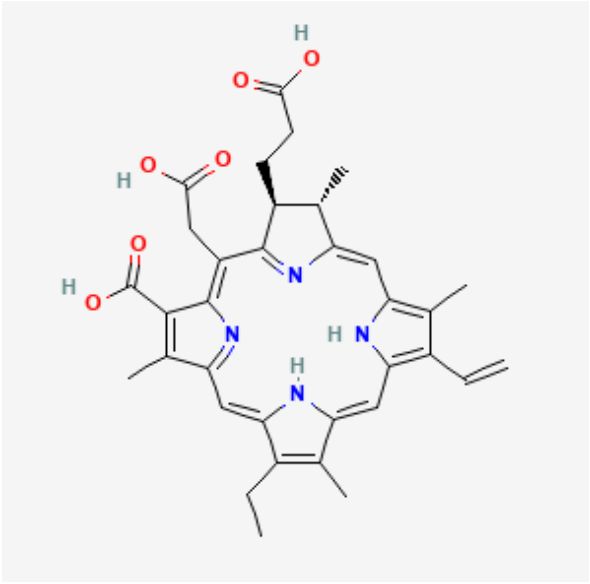

Figure 2.3 Chemical structure of Chlorin e6 [43].

Ce6 is a Food and Drug Administration-approved, second-generation, chlorine-based and anionic PS (Figure 2.3) [16]. It is known for the high amount of ROS generation due to absorption after 600-700 nm wavelength of light [16]. Antibacterial efficiency of Ce6 on different organisms such as *S. aureus* has been reported [17, 18, 19, 44]. Park *et al.* investigated the antibacterial efficiency of Ce6 on *S. aureus* both *in vitro* and *in vivo*. Their result indicated that Ce6-mediate PDT successfully inhibited bacterial viability on the skin infection model in mice [44]. Even though there are studies demonstrating the antibacterial potential of Ce6, there is a need for further investigation into bacterial periodontal disease models.

2.5 Light Sources

In PDT, light sources that emit light in the visible spectrum and near-infrared region are ideal for phototherapeutic purposes (Figure 2.4). Especially, the near-infrared region, between 750-2500 nm, has the highest tissue penetration making it suitable for deeper infections [34].

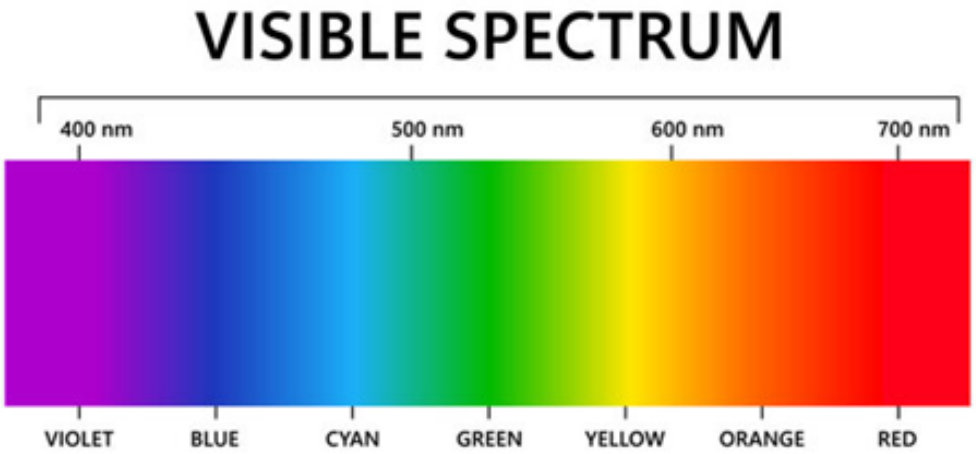

Figure 2.4 Visible spectrum region of the electromagnetic spectrum [45].

So far utilized light sources in PDT are non-coherent light sources (discharge lamps), lasers (yttrium and diode lasers), and lastly LEDs [34]. Lasers are very useful since they can produce focused beams of a specific wavelength for a variety of PS. Light can be easily focused on an area of interest by using optic fiber cables. In contrast to lasers, LEDs can not be coupled with optical fibers. However, their wider emission spectrum can be filtered to match with different PSs. In addition to that they are low in weight, making them portable and compact, also they can be found at lower prices [4, 46].

2.6 Biochemical Inactivation Mechanism of aPDT

PDT is a modality that was discovered more than 100 years ago [34]. Over these years, scientists established that the major reason for bacterial death in PDT is the oxidative damage caused by the reactive molecular species that PS produced through Type 1 and Type 2 reactions. Another known fact is that the electrostatic attraction between positively charged PS and the negatively charged biomolecules on the cellular wall favors cell killing [47]. After PDT, cells respond to structural damage with a rescue operation or by initiating cell death which both lead to apoptosis or necrosis [47, 48]. The first damage in the cell is highly dependent on the type and intracellular location of the PS upon irradiation. [48]. For example, mitochondrial photodamage generally initiates apoptosis by triggering the signaling pathways releasing cytochrome c and other apoptotic proteins [49]. Besides that, lysosomal photodamage is known to lead to apoptosis. Although the effect created by lysosomes is not as direct as in mitochondria, the release of several enzymes such as aSMase into the cytosol after irradiation and production of ceramide company apoptosis [47]. In the case of necrosis, cells undergo uncontrollable cell death. Although the role of necrosis is still not entirely clear, it generally causes the disintegration of cellular wall structures, swelling, and condensed nuclei [49]. It is anticipated that light energy and/or PS dosage tend to initiate cell death induced by necrosis.

PDT enhances the immunological response, which is another factor that coincides with bacterial cell death [49]. Although stimulation of T and B cells by the humoral immune system is more effective in the extermination of bacterial cells, studies are showing that the innate immune system can be triggered by PDT on the infection area [50, 51]. Also, it is known that ROS can trigger the AMPK signaling pathway to adjust the polarity of macrophages to an anti-inflammatory phenotype which consequently helps reduce the inflammation and promote wound healing [52].

3. MATERIAL AND METHOD

3.1 Bacterial strain

S. aureus ATCC 25923 (USA) strain was utilized in this study. To obtain single colonies, -80 °C frozen stock was seeded on a tryptic soy agar (TSA) plate by a scraper and incubated at 37 °C for 24 hours. The stock was kept at 4 °C and renewed every 2 weeks. For bacteria culture, a single colony was inoculated in the tryptic soy broth (TSB) and cultured overnight (18-20 hours) at 37°C in a shaking incubator at 200 rpm. Cells were harvested by centrifugation of 1 mL of overnight culture at 3000 rpm for 10 minutes (min) and the supernatant was discarded. The cell pellet was washed two times and resuspended in phosphate-buffered saline (PBS). The optical density of the bacterial suspension was measured with a UV-VIS spectrometer and the final concentration was adjusted to a range of $10^7 - 10^8$ colony-forming units per milliliter (CFU/mL).

3.2 Preparation of photosensitizer solutions

Ce6 (Cayman Chemicals, USA) and MB (ISOLAB Chemicals, Germany) were used in this study. 1 mM Ce6 and 1M MB stock solutions were prepared in PBS. By using 0.22 μm filters KCl solution was filtered and stored at 4 °C. Fresh solutions were prepared for each experiment and kept in the dark to prevent photobleaching. Absorption spectra of the PS solutions were assessed every two weeks.

3.3 Preparation of potassium chloride solution

A stock solution of 5M KCl solution was prepared in distilled water. The solution was filtered with 0.22 μm filters and stored at 4 °C. Fresh solutions were used for each

experiment.

3.4 Assessment of bacterial viability; Colony forming unit method

After the experiments, the bacterial viability of the suspensions were acquired by using the serial dilution method. 10 μL of aliquots of bacteria samples were diluted by 1/10 fold inside a 96-well plate. 30 μL of diluted samples were spread on TSA plates and incubated for 24 hours at 37 °C. CFUs were counted and multiplied by the dilution factor to assess the bacterial load on the corresponding plate.

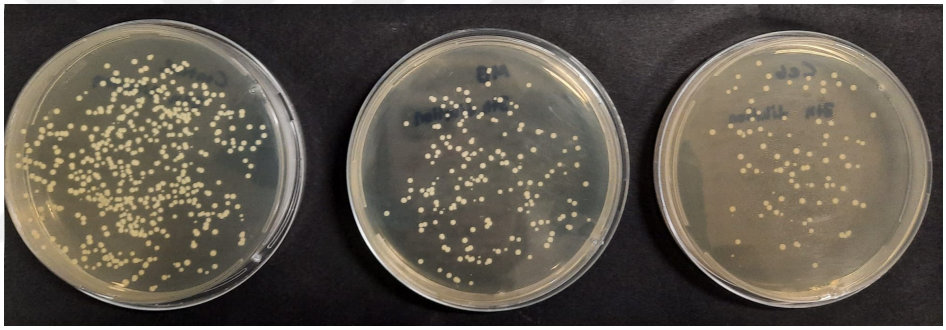

Figure 3.1 Images of colony forming units on TSA plates after PDT application.

3.5 Preparation of rough titanium discs

Commercially pure, 9 polished titanium discs were treated with sandblasting on one side (Figure 3.2). To prevent bacterial adhesion and to adhere discs to the well surface, untreated sides of the discs were covered with polydimethylsiloxane. Sizes of the discs were 15 mm in diameter and 2 mm in thickness and the same discs were used throughout the experiments. Before each experiment, discs were ultrasonically cleaned with acetone, absolute ethanol, and distilled water for 15 min then autoclaved for 15 min at 121 °C.

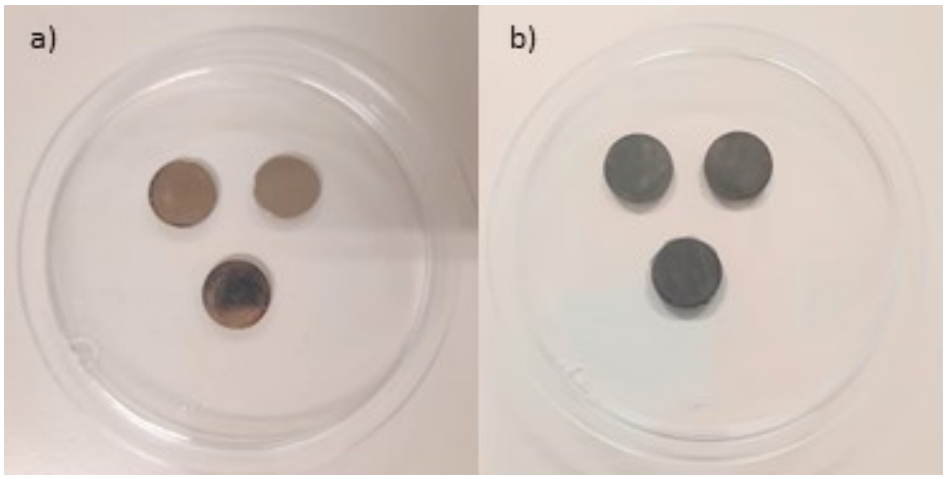

Figure 3.2 Images of a) polished and b) sandblasted titanium discs.

3.6 Roughness measurement of titanium discs

Roughness values of polished and sandblasted titanium discs were measured before and after the experiments by using Hirox, KH-8700 3D digital microscope. Arithmetic mean deviation of the assessed profile (Ra), maximum height of profile (Rz), and ten-point mean roughness (Rzjis, average of the absolute values of the five highest peaks and the five deepest valleys) were analyzed by the software of the device.

3.7 *In vitro* peri-implantitis model: Bacteria adhered on rough titanium disc.

S. aureus was cultured in TSB for 18-20 hours at 37 °C in a shaking incubator at 200 rpm. The culture was diluted in fresh TSB within a range of $10^7 - 10^8$ CFU/mL, supplemented with 200 μL of 50% glucose. Titanium discs were transfered into wells of a 12 well-plate, and 1.5 mL of TSB culture was dispensed into the wells (Figure 3.3). After the first 24 hours, 500 mL of fresh TSB was added into each well and bacteria were grown for another 24 hours at 37 °C. Before PDT applications, the discs were washed 2 times with 1 mL PBS to remove the planktonic or loosely adherent bacterial

cells.



Figure 3.3 Image of titanium discs placed on fresh bacterial broth solution before incubation for 48 hours.

3.8 Optical setup

A Thorlabs M660L4-C1 660 nm collimated LED light source was used throughout the experiments. The power density of the light source was adjusted to 100 mW/cm^2 using a power meter before each PDT application. 30 J/cm^2 and 60 J/cm^2 energy densities were applied to the wells by setting the irradiation times to 5 and 10 minutes.

3.9 Photodynamic therapy

Initially, we aimed to measure the dark toxicity of the PSs on *S. aureus* suspensions. Both Ce6 and MB experimental groups were formed as 0 (no treatment), 5, 10, 25, and 50 μM. Then, the effect of light was measured at 0 J/cm^2, 30 J/cm^2 and 60

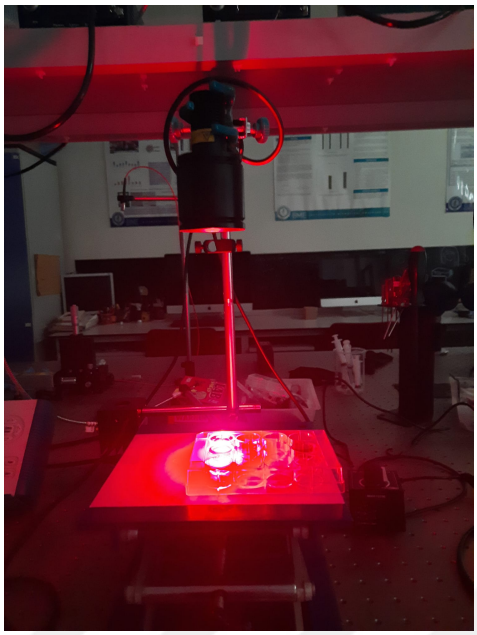

Figure 3.4 Image of a 660 nm collimated LED illuminating the 12 well-plate for the PDT application.

J/cm^2 at constant 100 mW/cm^2 power density. After these independent experiments, the optimum concentration of PSs and energy density were determined for the PDT groups as shown in Table 3.1 and Table 3.2. For the experiments, 1 mL of bacterial suspension was dispensed into wells for each group and repetition. In the no-treatment and only-light groups, bacterial suspensions were mixed with the same amount of PBS. In the PDT and dark toxicity groups, 1 mL of Ce6 and MB solutions were mixed with 1 mL of bacterial suspension. The mixed solutions were incubated for 15 minutes at 37 °C, then exposed to light (Figure 3.4). For the treatments conducted on *in vitro* PI model, bacteria-adhered discs were placed on 12 well-plates and incubated with 1 mL of Ce6 and MB with and without 400 mM KCl solution for 15 minutes at 37 °C. PS solutions were removed and discs were washed with PBS, then the discs were exposed to light. After treatments to disaggregate the clusters of bacteria, discs were placed in 1 mL PBS and cleaned in the ultrasonic bath for 15 min then vortexed for 1 min. Bacterial suspensions were serially diluted and CFUs were counted. The experiments were conducted at least three times.

Table 3.1
Parameters that will be applied on planktonic bacteria for the treatment groups of dark toxicity, light toxicity, and PDT

	Bacterial suspension	
Experimental groups	**PS concentration (μM)**	**Energy density (J/cm^2)**
Dark toxicity of Ce6	0,5,10,25,50	X
Dark toxicity of MB	0,5,10,25,50	X
Only light	X	30,60
Ce6 PDT	25	30,60
MB PDT	5	30

Table 3.2
Parameters that will be applied on the *in vitro* PI model for the treatment groups of PDT.

	***In vitro* peri-implantitis model**	
Experimental groups	**PS concentration (μM)**	**Energy density (J/cm^2)**
Ce6 PDT	25	60
MB PDT	5	30
Ce6 PDT+ 400 mM KCl	25	60
MB PDT+ 400 mM KCl	5	30

3.10 SEM analysis

After the experiments bacteria clusters on titanium discs were imaged using a Philips XL30 ESEM FEG instrument. Before imaging, specimens were fixed in 2.5% glutaraldehyde overnight at 4 °C and then dehydrated through 25%, 50%, 75%, and 100% ethanol. Finally, each disc was treated with hexamethyldisilazane solution before imaging.

3.11 Statistical analysis

The treatment outcomes were assessed by counting and normalizing the CFUs to the respective no-treatment control. The normalized data were analyzed using analysis of variance (ANOVA) and Dunnett's multiple comparison test. The groups that are statistically significantly different ($p<0.05$) were marked with a star (*).

4. RESULTS

4.1 Antibacterial effect of dark toxicity of Ce6 and MB on *S. aureus*

The dark toxicities of the PSs were evaluated at 5, 10, 25, and 50 μM concentrations. According to the results, the dark toxicity of Ce6 was lower than MB in each concentration. Normalized bacterial viability at 25 μM Ce6 was 90%. 25 μM MB reduced the viability to 6.5%. Based on the results represented in Figure 4.1 and Figure 4.2, the optimum concentrations of Ce6 and MB for further studies were determined as 25 μM and 5 μM, respectively as they did not cause significant toxicity on *S. aureus*.

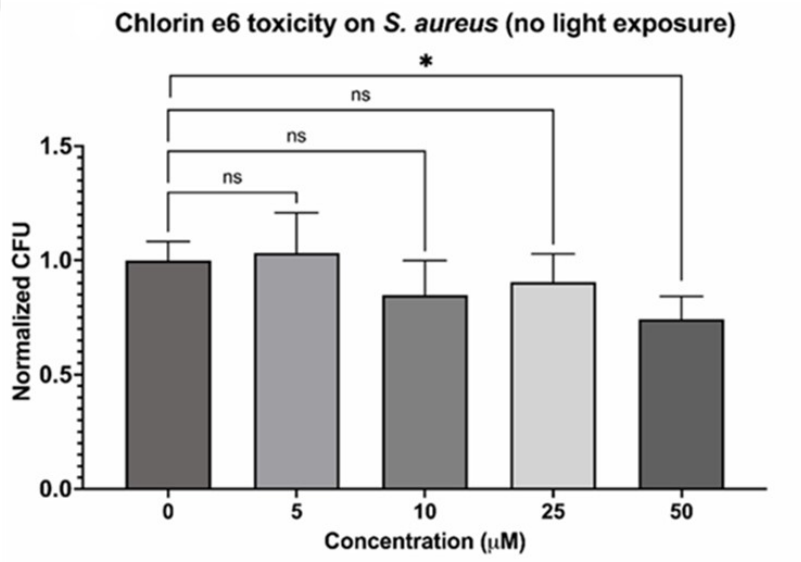

Figure 4.1 Antibacterial effect of dark toxicity of 0 μM, 5 μM,10 μM, 25 μM, and 50 μM Ce6 on *S. aureus*. The number of CFUs in each group was normalized with the no treatment (0 μM) group. (*: $p<0.05$, ns: not significant).

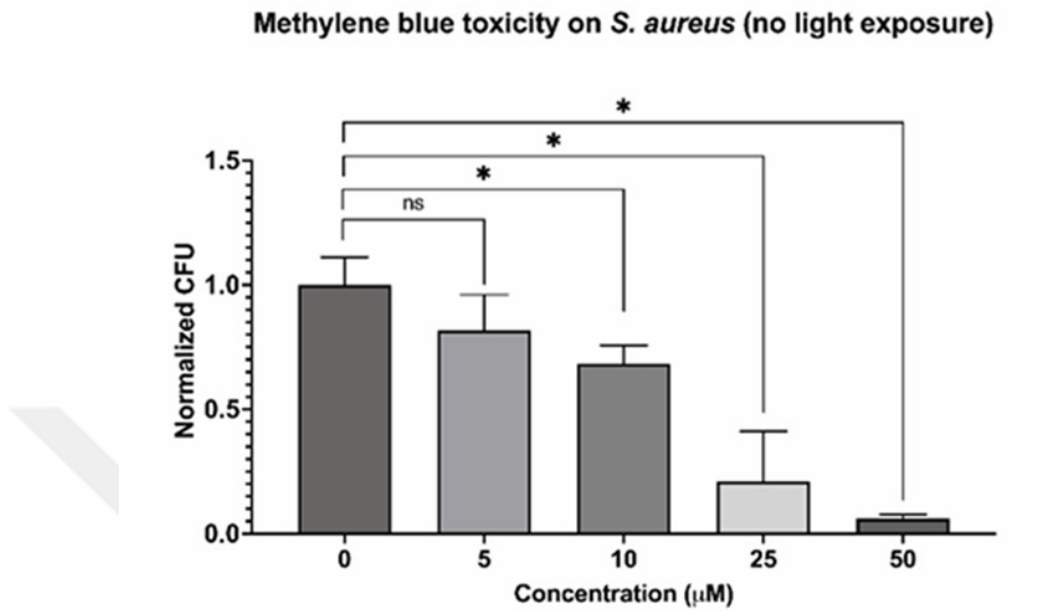

Figure 4.2 Antibacterial effect of dark toxicity of 0 μM, 5 μM,10 μM, 25 μM, and 50 μM MB on *S. aureus*. The number of CFUs in each group was normalized with the no treatment (0 μM) group. (*: $p<0.05$, ns: not significant).

4.2 Absorption spectra of Ce6 and MB

Absorption spectra of 25 μM Ce6 and 5 μM MB are shown in Figure 4.3. Both of the PSs have an absorption peak around 660 nm. After irradiation, the absorbance of the PSs was reduced.

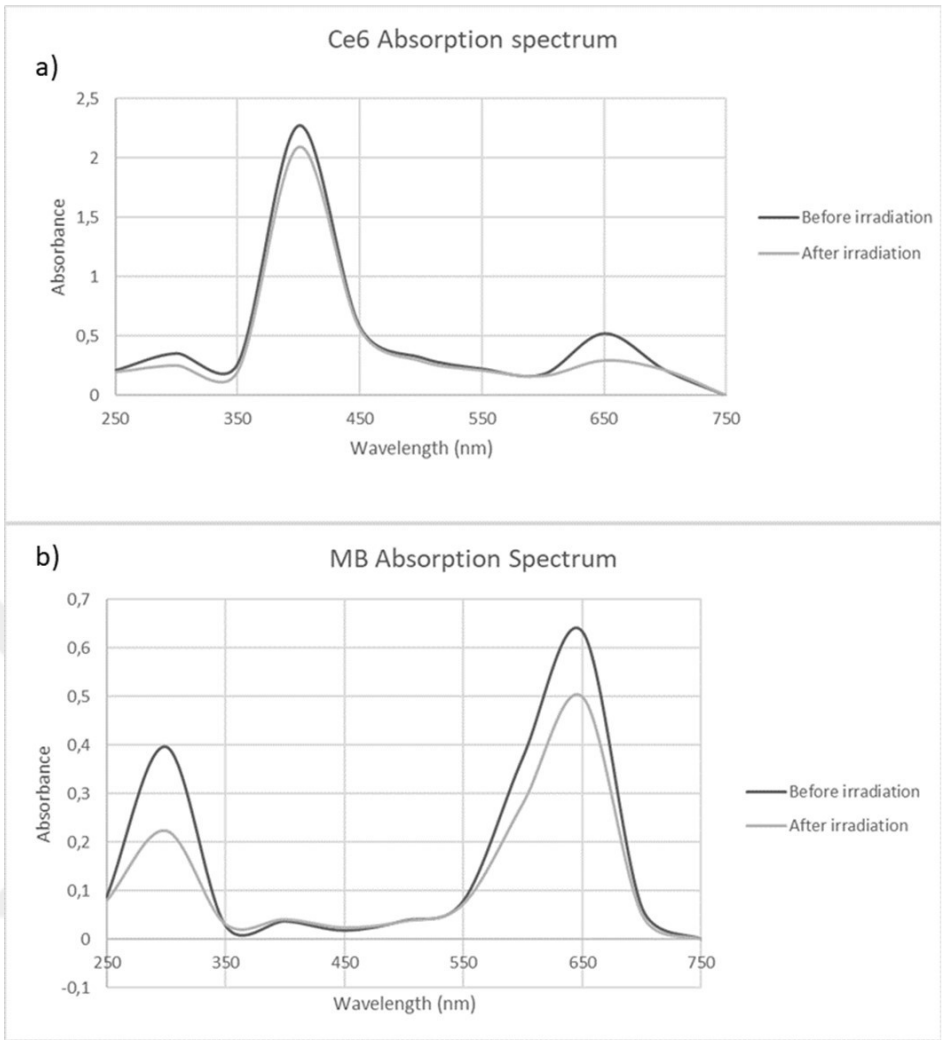

Figure 4.3 Absorption spectra of a) 25 μM Ce6 and b)5 μM MB before and after irradiation with 660 nm LED at 60 J/cm^2 and 30 J/cm^2 energy densities, respectively.

4.3 Antibacterial effect of 660 nm of light

To determine the effect of 660 nm LED irradiation, 100 mW/cm^2 power density was applied to the bacterial suspensions for 5 and 10 minutes to adjust the energy densities to 30 J/cm^2 and 60 J/cm^2, respectively. Both energy densities had no significant toxicity on *S. aureus*.

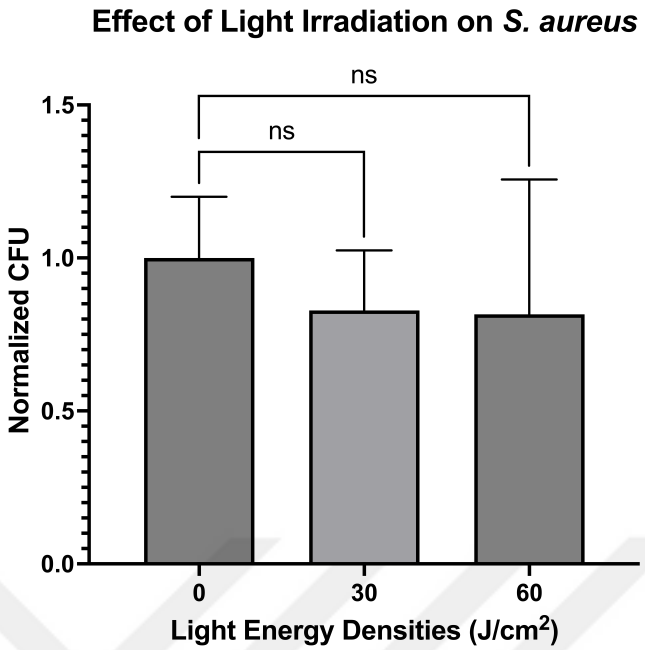

Figure 4.4 Effect of 660nm light irradiation on *S. aureus* suspensions at 100 mW/cm^2 power density. $0J/cm^2$, 30 J/cm^2 and 60 J/cm^2 energy densities were applied for 0, 5, and 10 minutes, respectively. The number of CFUs in each group was normalized with the no treatment group. (*: $p<0.05$, ns: not significant)

4.4 Antibacterial effect of Ce6 and MB-mediated PDT on planktonic bacteria

Ce6-mediated PDT was first tested on planktonic bacteria using 30 J/cm^2 and 60 J/cm^2 energy density. Normalized bacterial viability was reduced significantly in both of the PDT groups compared to the no-treatment group. There were no significant differences between different energy densities and 60 J/cm^2 energy density had the highest antibacterial effect as seen in Figure 4.5. At 30 J/cm^2, MB-mediated PDT significantly reduced the normalized bacterial viability and achieved a 99.9999% killing rate (Figure 4.6).

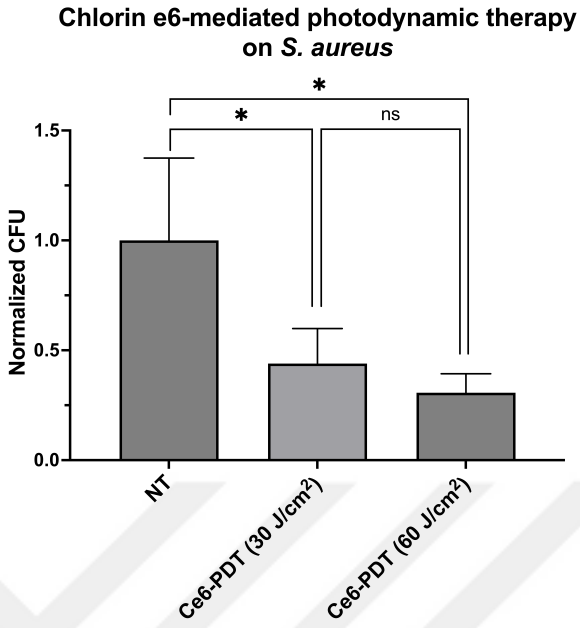

Figure 4.5 Antibacterial effect of 30 J/cm^2 and 60 J/cm^2 Ce6-mediated PDT on *S. aureus* suspensions. The number of CFUs in each group was normalized with the no treatment group. (*: $p<0.05$, ns: not significant)

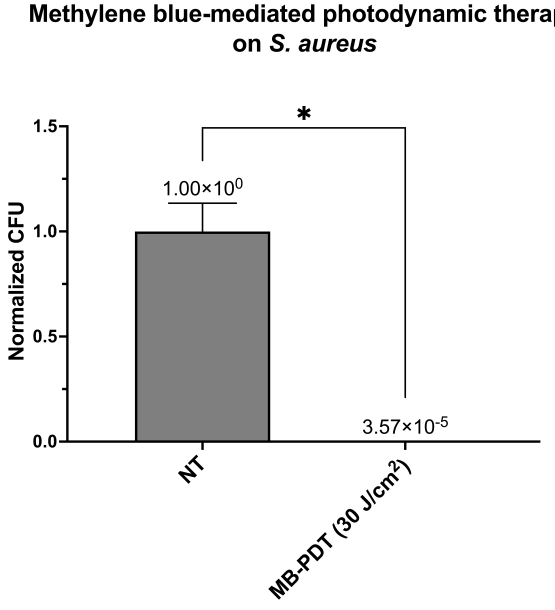

Figure 4.6 Antibacterial effect of 30 J/cm^2 MB-mediated PDT on *S. aureus* suspensions. The number of CFUs in each group was normalized with the no treatment group. (*: $p<0.05$, ns: not significant)

4.5 Antibacterial effect Ce6 and MB-mediated PDT on *in vitro* PI model

Both PDT groups significantly reduced the normalized bacterial viability compared to the no-treatment group. There were no statistical differences between the two PSs. The antibacterial effect of MB-mediated PDT was higher than Ce6 on titanium discs.

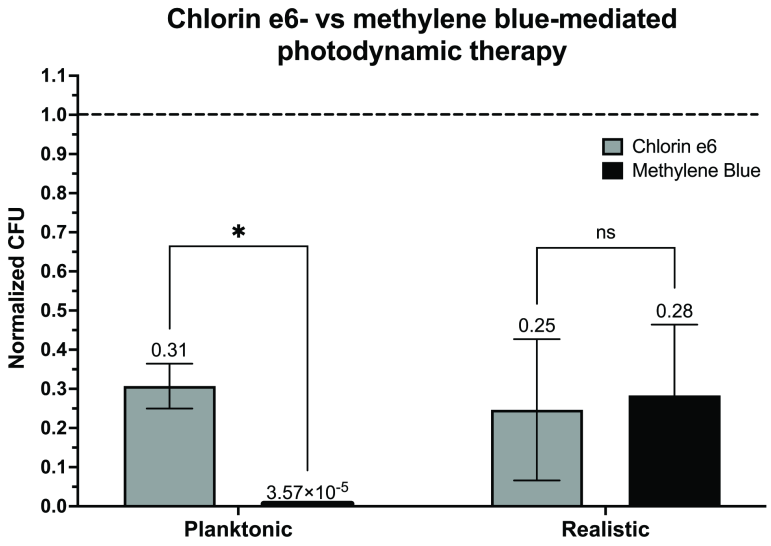

Figure 4.7 Antibacterial effect of 60 J/cm^2 Ce6-medieated PDT and 30 J/cm^2 MB-medieated PDT on *S. aureus* suspensions shown on the left. The antibacterial effect of 60 J/cm^2 Ce6-mediated PDT and 30 J/cm^2 MB-mediated PDT on *in vitro* PI model is shown on the right. The number of CFUs in each group was normalized with the no treatment group. (*: $p<0.05$, ns: not significant)

4.6 Antibacterial effect of the KCl addition to Ce6 and MB mediated PDT on *in vitro* PI model

Both of the PDT groups significantly reduced the normalized bacterial viability compared to the no-treatment group. There were no statistical differences between PDT groups. The antibacterial effect of Ce6-mediated PDT incubated with KCl was higher than MB and reached to 85% killing rate.

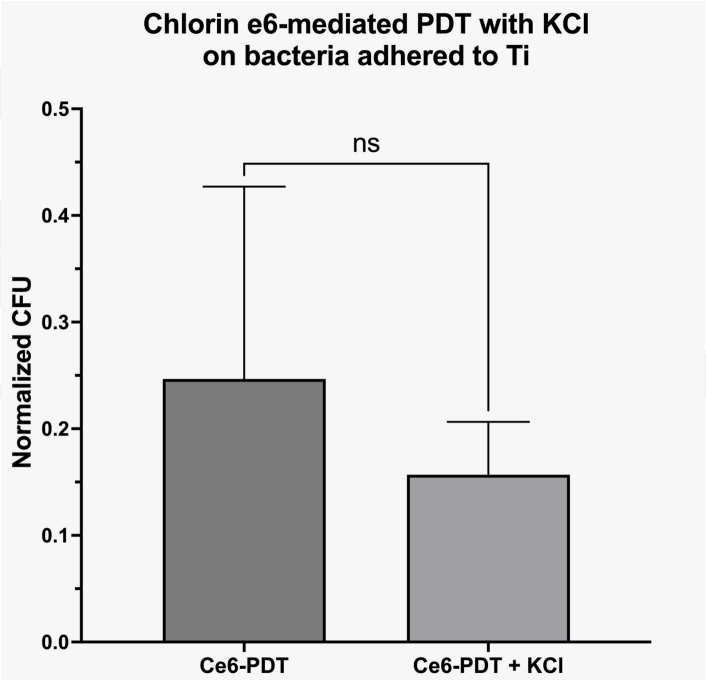

Figure 4.8 Antibacterial effect of 60 J/cm^2 Ce6-mediated PDT with and without 400 mM KCl on *in vitro* PI model. The number of CFUs in each group was normalized with the no treatment group. (*: $p<0.05$, ns: not significant)

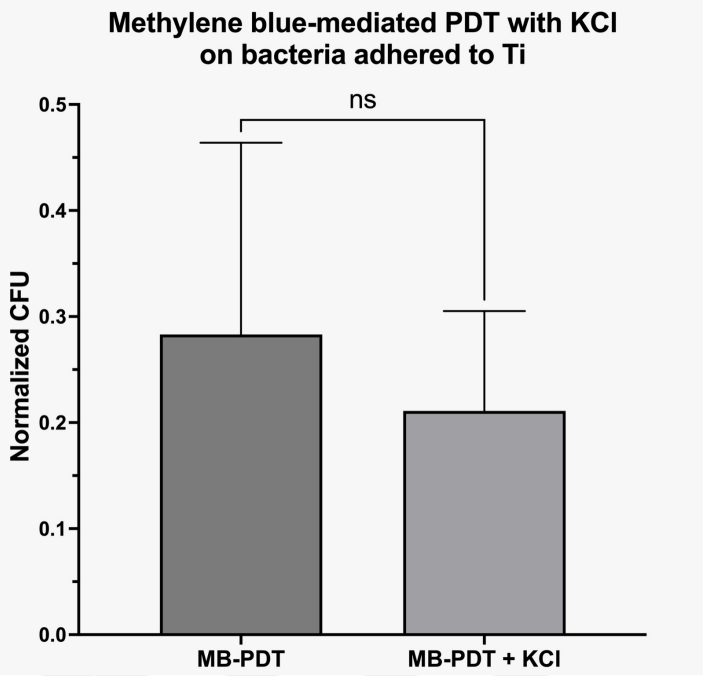

Figure 4.9 Antibacterial effect of 60 J/cm^2 MB-mediated PDT with and without 400 mM KCl on *in vitro* PI model. The number of CFUs in each group was normalized with the no treatment group. (*: $p<0.05$, ns: not significant)

4.7 Roughness measurements

The roughness measurements demonstrated that arithmetic mean deviation and maximum height of the profile in sandblasted titanium discs are higher than in polished titanium disc, as seen in Table 4.1. The 3D digital microscope images of the discs are presented in Figure 4.10.

Table 4.1
Roughness values of the polished and sandblasted discs measured with a 3D microscope.

	Polished disc	Rough disc 1	Rough disc 2	Rough disc 3
Ra, arithmetic mean deviation of the assessed profile (μm)	0,578	2,063	1,868	2,154
Ra, arithmetic mean deviation of the assessed profile (μm)	1,173	4,162	4,262	4,688
Ra, arithmetic mean deviation of the assessed profile (μm)	0,911	3,737	3,372	3,754

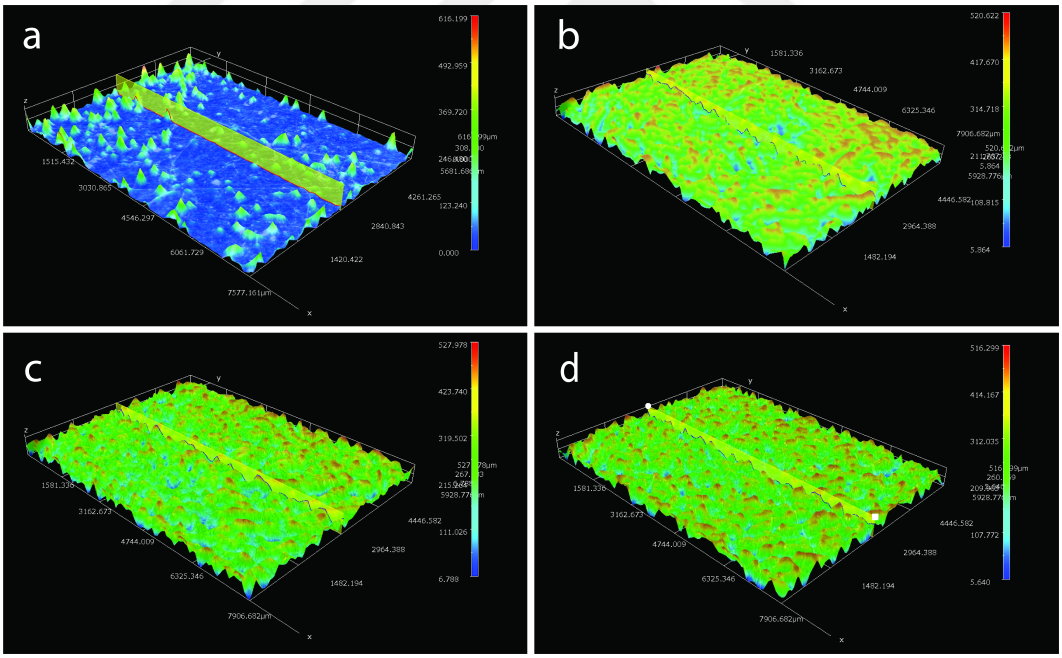

Figure 4.10 3D digital microscope images of random a) polished, and b) sandblasted titanium disc 1 and c) sandblasted titanium disc 2 and d) sandblasted titanium disc 3.

4.8 SEM analysis

The SEM images revealed the roughening of titanium discs, as well as the formation of clustering bacteria as shown in Figure 4.11. Bacteria after no treatment and Ce6- and MB-mediated PDT are shown in Figure 4.12. The effect of KCl administration on bacteria is shown in Figure 4.13.

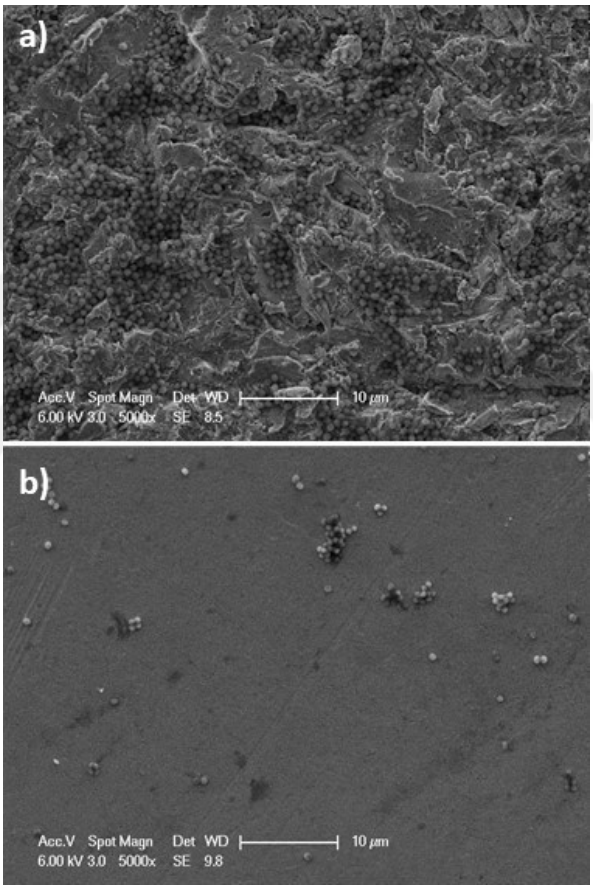

Figure 4.11 SEM images of bacteria forming clusters on a) sandblasted titanium disc and b) polished titanium disc.

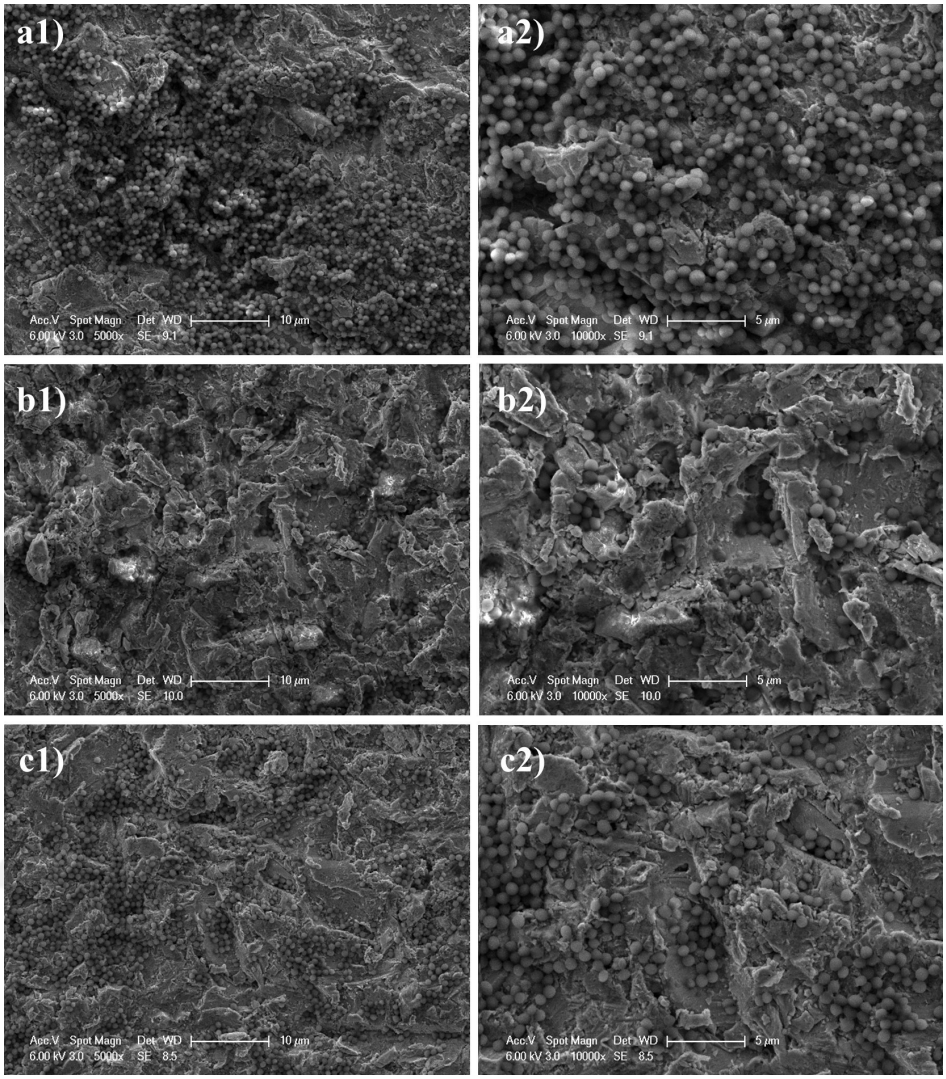

Figure 4.12 SEM images of bacteria on sandblasted titanium discs after no treatment at a1) 5000x magnification, a2) 10000x magnification; 25 μM Ce6 mediated PDT at b1) 5000x magnification, b2) 10000x magnification; 5 μM MB-mediated PDT at c1) 5000x magnification, c2) 10000x magnification at energy densities 0 J/cm^2, 30 J/cm^2 and 60 J/cm^2, respectively.

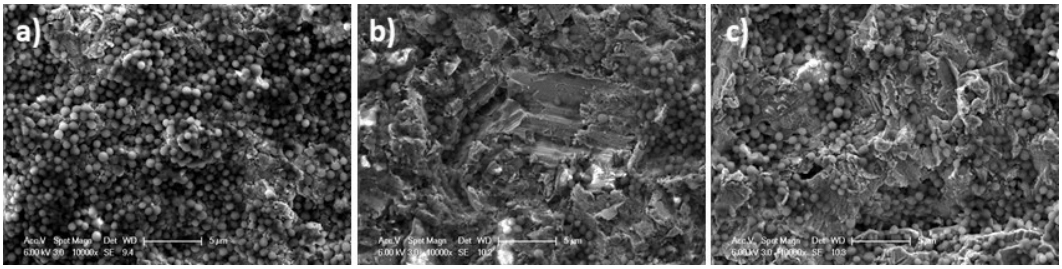

Figure 4.13 SEM images of bacteria on sandblasted titanium discs after a) no treatment, b) 25 μM Ce6 mediated PDT with the addition of KCl, c) 5 μM MB-mediated PDT with the addition of 400 mM KCl at energy densities 0 J/cm^2, 30 J/cm^2 and 60 J/cm^2, respectively.

5. DISCUSSION

Treatment of PI is a complex process and generally conventional treatments require supplementary approaches. One of the reasons which makes the treatment challenging is the surface roughness of dental implants. There is scientific evidence that the moderately rough surface of the implant promotes osteoblast differentiation which facilitates the osseointegration of the implant [53]. However, it is known that rough surfaces are more susceptible to bacterial adhesion, therefore, the disinfection of these surfaces is more challenging than smooth surfaces [54]. Besides conventional disinfection methods, antibacterial PDT has emerged as a promising and advantageous alternative to manage PI. PDT is less likely to promote resistance mechanisms on microorganisms and PS can be delivered locally to enhance the targeting sensitivity and to prevent systemic side effects. Although aPDT for PI has been studied with different PSs, there is a need for reliable protocols. Among all the PSs studied for PI, MB and TBO are the most common types. Another studied PS, for its antibacterial properties, is Ce6 which is known to have high photodynamic inactivation capacity. This study aimed to evaluate the Ce6-mediated aPDT for PI by comparing the results with MB-mediated protocol as a standard, in two *in vitro* models.

Initially, dark toxicity of Ce6 and MB and the effect of 660 nm light on planktonic *S. aureus* suspension were investigated. Concentrations of Ce6 at 5,10, and 25 μM, did not cause any toxicity on *S. aureus*. However, at 50 μM Ce6 bacterial viability was reduced significantly which can be seen in Figure 4.1. Dark toxicity of MB is significantly toxic on *S. aureus* at concentrations higher than 5 μM (Figure 4.2). Overall, MB was more toxic compared to the same concentrations of Ce6. Hence, the optimum concentrations of Ce6 and MB did not cause significant toxicity on *S. aureus* were determined as 25 μM and 5 μM, respectively. These results are around five times less than what Nie *et al.* study states as optimal concentrations of Ce6 and MB after evaluating their results with the related literature. After 5 and 10 min irradiation, light showed no significant toxicity on *S. aureus* suspension. In further experiments, 5

and 10 min irradiation was applied to the treatment groups, corresponding to 30 and 60 j/cm^2 energy density, respectively. In Figure 4.3, absorption spectra of 25 μM Ce6 and 5 μM MB show that after irradiation absorbance values were lower compared to initial which indicates the degradation of both PS molecules upon excitation.

After determining the concentrations of the PSs and light dosages, we aimed to compare the efficacy of Ce6-mediated PDT, with MB-mediated PDT on two *in vitro* models: planktonic bacteria and PI model. In the planktonic model, among all the groups, MB-mediated PDT at 30 j/cm^2 had the highest antibacterial effect and reached to 6-log decrease which corresponds to 99.9999% killing rate (Figure 4.6). Therefore, no further experiment using 60 j/cm^2 energy density was conducted for MB. Both of the Ce6-mediated PDT groups significantly eliminated the bacteria compared to no treatment group while the antibacterial effect was slightly better at 60 j/cm^2 as shown in Figure 4.5. Ce6-mediated PDT at 60 j/cm^2 on planktonic bacteria reached a 69% killing rate, almost 0.5-log reduction, even though the energy density and the PS concentration were higher than the MB group. Bishoff *et al.* showed the effects of Ce6 on different multi-drug resistant *S. aureus* strains by increasing incubation and irradiation time [55]. At a constant 30 min incubation time, they measured the effects of 1,5, and 10 min irradiation time at 30.6 mW/cm^2 power density. The authors demonstrated that, at 512 μM Ce6 (5 min incubation, 10 min irradiation) with the power density of 18.60 j/cm^2, the bacterial load is reduced by 3-log which corresponds to 99.9% killing rate. However, at lower concentrations such as 32 and 64 μM Ce6 caused a 0.7 log reduction of the bacterial load. Although they use a lower light dose and higher incubation time, the antibacterial effect of Ce6 on MRSA 44 strain at higher concentrations is close to the data presented in this thesis. Also, their results suggest that none of the concentrations exhibit significant dark toxicity, though they have not presented the accompanying data. In contrast to this, our results indicate that 50 μM Ce6 causes statistically significant toxicity on planktonic *S. aureus*.

In the *in vitro* PI model, we wanted to create a biofilm-like layer on a titanium surface that mimics the structure of a moderately rough dental implant surface. We successfully roughened the surface by sandblasting one side of the titanium discs to increase the clustered and surface-associated bacteria number as seen on the SEM images in Figure 4.11a. The Ra value of three random sandblasted discs was 2.028 μm on average which was desirable since the Ra value of the commercially available dental implants spans between 1 and 2 μm, classified as moderately rough surface [56].

It is well known that planktonic bacteria are more susceptible to PDT than biofilm bacteria [25]. In parallel with this knowledge, our results demonstrated that the bacteria were less susceptible to MB-mediated PDT in the PI model. Normalized bacterial viability after the MB-mediated PDT was increased drastically compared to the planktonic model. As seen in Figure 4.7, the killing rate of MB reached 72% which approximately corresponds to a 0.55-log reduction ($p<0,05$). Although there were no statistically significant differences between the two Ce6 models, killing rate of Ce6-mediated PDT was 6% more efficient in the titanium PI model and caused almost 0.65-log reduction. Nie *et al.* achieved an almost 2-log reduction of the bacteria load in S. mutans biofilms with 25 μM Ce6 and MB at 15 j/cm^2 energy density. When they increased the concentration to 200 μM Ce6, PDT was more effective and reached a 5-log reduction of bacteria while the same concentration MB could not reach significant phototoxicity. In another study, Park *et al.* investigated the effect of Ce6-mediated PDT on *S. aureus* Xen29 which is a bioluminescent strain of *S. aureus* ATCC25923. They conducted both *in vitro* and *in vivo* studies with a 664 nm laser for skin infection. To measure biofilm viability, they used the crystal violet staining technique and measured the absorbance of biofilms. Their result demonstrated that 10 μM Ce6 at 10 j/cm^2 light significantly reduced the biofilm formation [42]. Overall, the antibacterial effect of Ce6 in both of the *in vitro* models remained lower when we compared our results with these similar studies. It should be noted that, in these studies, light is applied either on a biofilm incubated on the surface of a well-plate, generally made from polystyrene, or to disassociated biofilm bacteria. However, unlike these mentioned studies, we applied the light directly on bacteria-adhered titanium surfaces. Even though both PDT protocols were efficient at eradicating the bacteria clusters, results show that complete

disinfection can not be achieved. Bacteria that reside inside the pits were hard to reach and have the possibility of reduced treatment outcomes. Visual examination of the SEM images in Figure 4.12 and Figure 4.13 also suggests that both Ce6 and MB-mediated PDT groups had fewer bacteria on the surface compared to the no-treatment groups. However, bacteria were present in the deeper parts of the discs. Although PDT is a minimally invasive method, we applied PDT only for one time. So, it can be applied repeatedly until achieving satisfactory results.

Our research group has recently showed that 400 mM KCl does not cause toxicity on either *S. aureus* or mouse fibroblast cells and potentiates the effect of Ce6-mediated PDT on planktonic bacteria [22]. Building on these findings by our group, this study aimed to demonstrate the same effect of KCl for the first time on bacteria adhered to titanium discs as an *in vitro* model for PI. The results in Figure 4.8 revealed that the most successful treatment protocol for the *in vitro* PI model was Ce6-mediated PDT, with around an 85% killing rate. Although not statistically significant ($p=0.45$), the efficacy of Ce6-mediated PDT increased by around 9% when the bacteria were incubated with 400 mM KCl. On the other hand, the efficacy of MB-mediated PDT increased by about 7% with 400 mM KCl. Wen *et al.* explained the effect of potassium iodide was due to the PDT-induced oxidation of iodide producing two types of antibacterial molecules: molecular iodide and short-lived iodide species. In our study, we could not demonstrate the underlying mechanism of the antibacterial effect of KCL. However, our research group showed that KCl has no toxicity on *S. aureus* therefore the antibacterial effect could be due to the phototoxicity [22].

An important limitation of this study is that we utilized mono-species biofilm to create a clinical model which is considerably different from the actual environment of PI. In the clinical case, the biofilm is composed of several oral bacteria species and the implant is anchored to bone and soft tissue with a different structure. Another restriction is that *S. aureus* is a gram-positive bacteria that uptakes anionic PSs more easily than gram-negative bacteria. Therefore, the addition of gram-negative bacteria and multi-species biofilm can increase the impact of this study. Since this study is strictly performed *in vitro*, the toxicity of light on osteoblast and fibroblast cells as

well as the effect of light on surface roughness should be investigated for future *in vivo* studies.

To sum up, a noteworthy result in this study is that Ce6-mediated PDT on bacteria adhered to titanium discs was as effective as planktonic bacteria. In other words, the efficacy of Ce6-mediated PDT was not negatively affected due to the cluster formation and surface adhesion of bacteria as MB-mediated protocol did. The same light source was used to excite both PSs throughout the study, therefore, it is not expected that any differences in the treatment outcome are due to the wavelength of the light used. The uptake and activation of the PSs are expected to be more difficult for bacteria that adhere to surfaces and form clusters than in planktonic conditions. Therefore, the low effectiveness of MB-mediated PDT on surface-attached bacteria may be attributed to the relatively low PS and energy density used in the experiments. Differences in the chemical structures of the two PSs may also have affected the interaction of these PSs with bacteria in the two different models.

6. CONCLUSION

To conclude, our data suggest that Ce6-mediated PDT is as effective as MB-mediated PDT and effectively clean bacteria from the titanium surface. In addition to that, the efficacy of Ce6 is consistent in both of the *in vitro* models, unlike MB. The present findings of this study are promising to treat PI. Still, further studies are needed to produce effective and reproducible PDT protocols to be used in *in vivo* studies and further in clinical applications.

REFERENCES

1. Peres, M. A., L. M. D. Macpherson, R. J. Weyant, B. Daly, R. Venturelli, M. R. Mathur, S. Listl, R. K. Celeste, C. C. Guarnizo-Herreño, C. Kearns, H. Benzian, P. Allison, and R. G. Watt, "Oral diseases: a global public health challenge," Vol. 394, no. 10194, pp. 249–260.

2. Petersen, P. E., D. Bourgeois, H. Ogawa, S. Estupinan-Day, and C. Ndiaye, "The global burden of oral diseases and risks to oral health," Vol. 83, no. 9, pp. 661–669.

3. Rokaya, D., V. Srimaneepong, W. Wisitrasameewon, M. Humagain, and P. Thunyakitpisal, "Peri-implantitis update: Risk indicators, diagnosis, and treatment," Vol. 14, no. 4, pp. 672–682.

4. Veerachamy, S., T. Yarlagadda, G. Manivasagam, and P. K. Yarlagadda, "Bacterial adherence and biofilm formation on medical implants: a review," Vol. 228, no. 10, pp. 1083–1099.

5. Ramanauskaite, A., T. Fretwurst, and F. Schwarz, "Efficacy of alternative or adjunctive measures to conventional non-surgical and surgical treatment of peri-implant mucositis and peri-implantitis: a systematic review and meta-analysis," Vol. 7, no. 1, p. 112.

6. Dougherty, T. J., C. J. Gomer, B. W. Henderson, G. Jori, D. Kessel, M. Korbelik, J. Moan, and Q. Peng, "Photodynamic therapy," Vol. 90, no. 12, pp. 889–905.

7. Garcia de Carvalho, G., J. C. Sanchez-Puetate, N. Casalle, E. Marcantonio Junior, and D. Leal Zandim-Barcelos, "Antimicrobial photodynamic therapy associated with bone regeneration for peri-implantitis treatment: A case report," Vol. 30, p. 101705.

8. Alasqah, M. N., "Antimicrobial efficacy of photodynamic therapy on dental implant surfaces: A systematic review of in vitro studies," Vol. 25, pp. 349–353.

9. Ghanem, A., S. Pasumarthy, V. Ranna, S. V. Kellesarian, T. Abduljabbar, F. Vohra, and H. Malmstrom, "Is mechanical curettage with adjunct photodynamic therapy more effective in the treatment of peri-implantitis than mechanical curettage alone?," Vol. 15, pp. 191–196.

10. Tim, M., "Strategies to optimize photosensitizers for photodynamic inactivation of bacteria," Vol. 150, pp. 2–10.

11. Yu, J., C.-H. Hsu, C.-C. Huang, and P.-Y. Chang, "Development of therapeutic au-methylene blue nanoparticles for targeted photodynamic therapy of cervical cancer cells," Vol. 7, no. 1, pp. 432–441.

12. Huang, L., T. Dai, and M. R. Hamblin, "Antimicrobial photodynamic inactivation and photodynamic therapy for infections," Vol. 635, pp. 155–173.

13. Yin, X., Z. Fang, Y. Fang, L. Zhu, J. Pang, T. Liu, Z. Zhao, and J. Zhao, "Antimicrobial photodynamic therapy involving a novel photosensitizer combined with an antibiotic in the treatment of rabbit tibial osteomyelitis caused by drug-resistant bacteria," Vol. 13, p. 876166.

14. de Almeida, J. M., L. H. Theodoro, A. F. Bosco, M. J. H. Nagata, M. Oshiiwa, and V. G. Garcia, "Influence of photodynamic therapy on the development of ligature-induced periodontitis in rats," Vol. 78, no. 3, pp. 566–575.

15. Kim, T. E., and J.-E. Chang, "Recent studies in photodynamic therapy for cancer treatment: From basic research to clinical trials," Vol. 15, no. 9, p. 2257.

16. Hak, A., M. S. Ali, S. A. Sankaranarayanan, V. R. Shinde, and A. K. Rengan, "Chlorin e6: A promising photosensitizer in photo-based cancer nanomedicine," Vol. 6, no. 2, pp. 349–364.

17. Nie, M., D. M. Deng, Y. Wu, K. T. de Oliveira, V. S. Bagnato, W. Crielaard, and A. N. d. S. Rastelli, "Photodynamic inactivation mediated by methylene blue or chlorin e6 against streptococcus mutans biofilm," Vol. 31, p. 101817.

18. Nie, M., R. C. E. Silva, K. T. de Oliveira, V. S. Bagnato, A. N. de Souza Rastelli, W. Crielaard, J. Yang, and D. M. Deng, "Synergetic antimicrobial effect of chlorin e6 and hydrogen peroxide on multi-species biofilms," Vol. 37, no. 6, pp. 656–665.

19. Avşar, N. T., E. Bakay, and A. Kolkıran, "Photodynamic action of chlorin e6 against methicillin resistant staphylococcus aureus with the aid of ethanol," Vol. 5, no. 3, pp. 100–105. Number: 3 Publisher: Mustafa HASBAHÇECİ.

20. Nakonechny, F., M. Barel, A. David, S. Koretz, B. Litvak, E. Ragozin, A. Etinger, O. Livne, Y. Pinhasi, G. Gellerman, and M. Nisnevitch, "Dark antibacterial activity of rose bengal," Vol. 20, no. 13, p. 3196.

21. Wen, X., X. Zhang, G. Szewczyk, A. El-Hussein, Y.-Y. Huang, T. Sarna, and M. R. Hamblin, "Potassium iodide potentiates antimicrobial photodynamic inactivation mediated by rose bengal in in vitro and in vivo studies," Vol. 61, no. 7, pp. e00467–17.

22. Özhan, H., E. Saraç, E. S. Ceylan, and M. K. Ruhi, "Potassium chloride potentiates chlorin e6-mediated antimicrobial photodynamic inactivation," in *2023 Medical Technologies Congress (TIPTEKNO)*, pp. 1–4, 2023.

23. Kim, H.-S., E. J. Cha, H.-J. Kang, J.-H. Park, J. Lee, and H.-D. Park, "Antibacterial application of covalently immobilized photosensitizers on a surface," Vol. 172, pp. 34–42.

24. P, D., S. Dn, W. B, C. Cl, L. Km, L. Cb, F. Kp, N. Dk, and I. M, "Contemporary approaches and future perspectives of antibacterial photodynamic therapy (aPDT) against methicillin-resistant staphylococcus aureus (MRSA): A systematic review," Vol. 200.

25. Gordon, V. D., and L. Wang, "Bacterial mechanosensing: the force will be with you, always," *Journal of Cell Science*, Vol. 132, p. jcs227694, 04 2019.

26. Gonzalo, E., L. J. G. Villagra, B. Miegimolle, and M. J. Suarez, "What is the prevalence of peri-implantitis? a systematic review and meta-analysis," Vol. 22, no. 1, p. 449.

27. Rakic, M., M. G. Grusovin, and L. Canullo, "The microbiologic profile associated with peri-implantitis in humans: A systematic review," Vol. 31, no. 2, pp. 359–368.

28. Persson, G. R., and S. Renvert, "Cluster of bacteria associated with peri-implantitis," Vol. 16, no. 6, pp. 783–793.

29. Secgin-Atar, A., G. Aykol-Sahin, N. A. Kocak-Oztug, F. Yalcin, A. Gokbuget, and U. Baser, "Evaluation of surface change and roughness in implants lost due to peri-implantitis using erbium laser and various methods: An in vitro study," Vol. 11, no. 10, p. 2602.

30. Renvert, S., A.-M. Roos-JansÃ¥ker, and N. Claffey, "Non-surgical treatment of peri-implant mucositis and peri-implantitis: a literature review," Vol. 35, no. 8, pp. 305–315.

31. Stewart, P. S., "Mechanisms of antibiotic resistance in bacterial biofilms," Vol. 292, no. 2, pp. 107–113.

32. A, M.-V., B.-V. P, S.-R. Mf, and F.-G. Jc, "Decontamination of dental implant surface in peri-implantitis treatment: a literature review," Vol. 18, no. 6.

33. Liu, J. X., J. Werner, T. Kirsch, J. D. Zuckerman, and M. S. Virk, "Cytotoxicity evaluation of chlorhexidine gluconate on human fibroblasts, myoblasts, and osteoblasts," Vol. 3, no. 4, pp. 165–172.

34. Keshaw, D. K., *Photodynamic Therapy An Overview Of Fundamentals Functioning And Clinical Application In The Treatment Of Periodontal Disease*, BFC Publications. Google-Books-ID: aJe1EAAAQBAJ.

35. Passanezi, E., C. A. Damante, M. L. R. de Rezende, and S. L. A. Greghi, "Lasers in periodontal therapy," Vol. 67, no. 1, pp. 268–291.

36. Kwiatkowski, S., B. Knap, D. Przystupski, J. Saczko, E. Kędzierska, K. Knap-Czop, J. Kotlinska, O. Michel, K. Kotowski, and J. Kulbacka, "Photodynamic therapy - mechanisms, photosensitizers and combinations," Vol. 106, pp. 1098–1107.

37. Hamblin, M., and Y. Huang, *Handbook of Photomedicine*, Taylor & Francis, 2013.

38. Calixto, G. M. F., J. Bernegossi, L. M. de Freitas, C. R. Fontana, and M. Chorilli, "Nanotechnology-based drug delivery systems for photodynamic therapy of cancer: A review," Vol. 21, no. 3, p. 342.

39. Y, L., Q. R, Z. Saj, B. E, and H. M, "Antibacterial photodynamic therapy: overview of a promising approach to fight antibiotic-resistant bacterial infections," Vol. 1, no. 3.

40. Josefsen, L. B., and R. W. Boyle, "Photodynamic therapy and the development of metal-based photosensitisers," Vol. 2008, p. 276109.

41. Allison, R. R., G. H. Downie, R. Cuenca, X.-H. Hu, C. J. Childs, and C. H. Sibata, "Photosensitizers in clinical PDT," Vol. 1, no. 1, pp. 27–42.

42. Correia, J. H., J. A. Rodrigues, S. Pimenta, T. Dong, and Z. Yang, "Photodynamic therapy review: Principles, photosensitizers, applications, and future directions," Vol. 13, no. 9, p. 1332.

43. PubChem, "18-(2-carboxyethyl)-20-(carboxymethyl)-12-ethenyl-7-ethyl-3,8,13,17-tetramethyl-17,18,22,23-tetrahydroporphyrin-2-carboxylic acid."

44. Park, J.-H., M.-Y. Ahn, Y.-C. Kim, S.-A. Kim, Y.-H. Moon, S.-G. Ahn, and J.-H. Yoon, "In vitro and in vivo antimicrobial effect of photodynamic therapy using a highly pure chlorin e6 against staphylococcus aureus xen29," Vol. 35, no. 4, pp. 509–514.

45. Montaseri, H., C. A. Kruger, and H. Abrahamse, "Inorganic nanoparticles applied for active targeted photodynamic therapy of breast cancer," Vol. 13, no. 3, p. 296.

46. Brancaleon, L., and H. Moseley, "Laser and non-laser light sources for photodynamic therapy," Vol. 17, no. 3, pp. 173–186.

47. Sabino, C. P., M. S. Ribeiro, M. Wainwright, C. Dos Anjos, F. P. Sellera, M. Dropa, N. B. Nunes, G. T. P. Brancini, G. U. L. Braga, V. E. Arana-Chavez, R. O. Freitas, N. Lincopan, and M. S. Baptista, "The biochemical mechanisms of antimicrobial photodynamic therapy," Vol. 99, no. 2, pp. 742–750.

48. Ac, M., "Signaling pathways in cell death and survival after photodynamic therapy," Vol. 57, no. 1. Publisher: J Photochem Photobiol B.

49. Sorrin, A. J., M. Kemal Ruhi, N. A. Ferlic, V. Karimnia, W. J. Polacheck, J. P. Celli, H.-C. Huang, and I. Rizvi, "Photodynamic therapy and the biophysics of the tumor microenvironment," Vol. 96, no. 2, pp. 232–259.

50. Reginato, E., P. Wolf, and M. R. Hamblin, "Immune response after photodynamic therapy increases anti-cancer and anti-bacterial effects," Vol. 4, no. 1, pp. 1–11.

51. Huang, Y.-Y., M. Tanaka, D. Vecchio, M. Garcia-Diaz, J. Chang, Y. Morimoto, and M. R. Hamblin, "Photodynamic therapy induces an immune response against a bacterial pathogen," Vol. 8, no. 5, pp. 479–494.

52. H, C., W. L, W. T, Z. F, S. J, F. J, K. X, and S. J, "PTT/ PDT-induced microbial apoptosis and wound healing depend on immune activation and macrophage phenotype transformation," Vol. 167.

53. Teughels, W., N. Van Assche, I. Sliepen, and M. Quirynen, "Effect of material characteristics and/or surface topography on biofilm development," Vol. 17 Suppl 2, pp. 68–81.

54. Leonhardt, A., C. Bergström, and U. Lekholm, "Microbiologic diagnostics at titanium implants," Vol. 5, no. 4, pp. 226–232.

55. Winkler, K., C. Simon, M. Finke, K. Bleses, M. Birke, N. Szentmàry, D. Hüttenberger, T. Eppig, T. Stachon, A. Langenbucher, H.-J. Foth, M. Herrmann, B. Seitz, and M. Bischoff, "Photodynamic inactivation of multidrug-resistant staphylococcus aureus by chlorin e6 and red light (Î»=670nm)," Vol. 162, pp. 340–347.

56. Nicolas-Silvente, A. I., E. Velasco-Ortega, I. Ortiz-Garcia, L. Monsalve-Guil, J. Gil, and A. Jimenez-Guerra, “Influence of the titanium implant surface treatment on the surface roughness and chemical composition,” Vol. 13, no. 2, p. 314.